Investigations of a r.f. stored Ca+ ion cloud and observation of the S-D forbidden transitions

M. Knoop, M. Vedel, F. Vedel

Classification
Physics Abstracts
32.70F — 32.80B — 35.80

Investigations of a r.f. stored Ca^+ ion cloud and observation of the S-D forbidden transitions

M. Knoop, M. Vedel and F. Vedel

Physique des Interactions Ioniques et Moléculaires (*), Université de Provence, Case C21, 13397 Marseille Cedex 20, France

(*Received 31 May 1994, accepted in final form 13 July 1994*)

Résumé. — Afin d'explorer les possibilités d'un étalon de fréquence dans le domaine optique (729 nm), un nuage d'ions Ca^+ est piégé dans un dispositif de Paul de dimension intermédiaire. De longues durées d'observation sont obtenues en présence d'hélium dans un domaine de pression autour de 10^{-6}-10^{-8} mbar et dans un puits de pseudopotentiel de 62 eV. Les premières observations de la transition quadrupolaire électrique ont été obtenues par le peuplement direct du niveau métastable correspondant ($\tau \approx 1$ s). L'utilisation d'une diode laser accordable en cavité étendue permettant de sonder les deux niveaux, alors que seulement l'un des deux était initialement peuplé a montré des intensités des fluorescences correspondantes du même ordre, indiquant la présence, à côté de la relaxation collisionnelle, de très forts mélanges des niveaux fins.

Abstract. — In order to exploit the capability of a high-Q transition for a frequency standard in the optical domain (729 nm), a stored Ca^+ ion cloud in a medium-size ion trap is investigated. Long confinement times are obtained in the presence of helium as a buffer gas in the range 10^{-6}-10^{-8} mbar and at a pseudopotential well depth of 62 eV. First observations of the electric quadrupole line were achieved by direct excitation of one of the first metastable doublet levels ($\tau \approx 1$ s). Utilisation of a grating-stabilised diode laser in order to probe both levels when only one level is initially populated allows us to observe almost equal fluorescence intensities of both forbidden lines that show the presence of a strong fine structure mixing which exists in addition to quenching.

1. Introduction.

Radiofrequency traps are efficient tools for developing new frequency standards [1, 2]. Such devices exceed, in the micrometric domain, the long term stability properties of cesium clocks [3]. Indeed, the most important cause of line broadening (first-order Doppler effect) does not exist in ion traps when wavelengths are of the same order of magnitude as the ion motion amplitude (Lamb-Dicke regime) [4]. Laser cooling extends this property to the optical region as demonstrated in [5], where an effective line quality factor ($Q = \nu/\Delta\nu$) of 10^{13} was achieved on the electric quadrupole UV line of HgII at 281 nm. The very long-lived D levels of BaII (49 s for $D_{3/2}$ [6] and 34.5 s for $D_{5/2}$ [7]) provide another candidate. The corresponding

(*) URA CNRS 773.

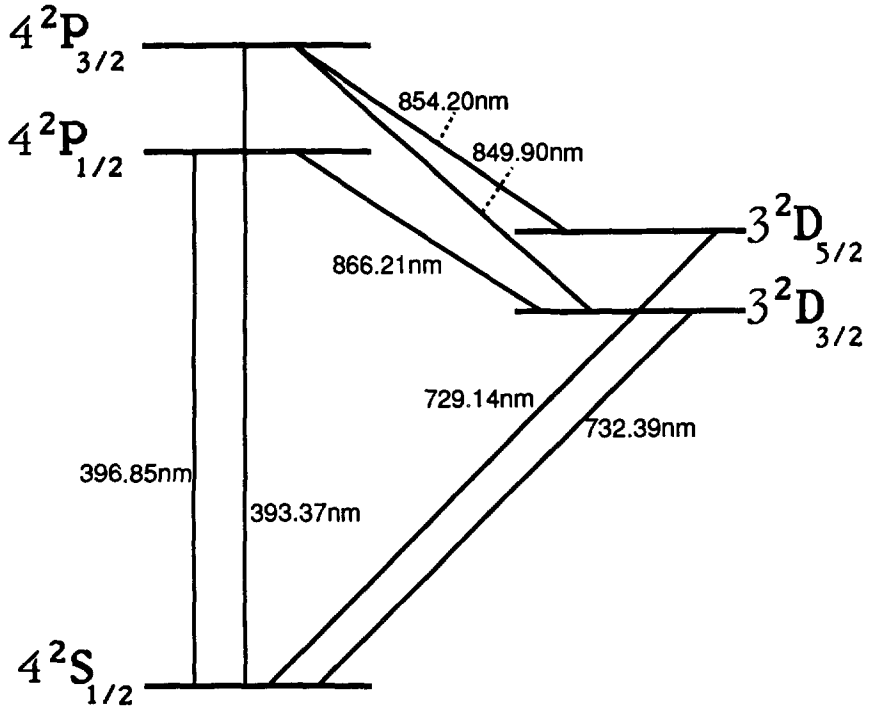

Fig. 1. — First energy levels of CaII.

$6^2S_{1/2}$-$5^2D_{5/2}$ i.r. transition at 1.76 μm with a natural linewidth of 5 mHz was investigated on a single laser cooled ion where a linewidth of 13 kHz was observed [8], while the absolute frequency of the magnetic dipolar transition at 12.48 μm was measured on a single laser-cooled ion with a linewidth of 11 kHz [9]. Other possibilities exist with alkaline-earth ions because of their similar Λ energy level scheme, for instance Yb^+ at 411 nm [10], which also has a long-lived metastable D-level ($\tau(5D_{3/2}) = 20$ ms [11]).

Among several candidates for optical frequency standards using the technique of ion storage, Ca^+ appears to be one of the most promising [12, 13]. The forbidden line $4^2S_{1/2}$-$3^2D_{5/2}$ at 729 nm (Fig. 1) allows the prediction of a Q factor superior to 10^{14} Linewidth broadening due to the Zeeman effect can be avoided in $^{43}Ca^+$ because of the existence of a transition which, due to its nuclear spin of 7/2, is independent (to first order) of magnetic fields. Laser cooling must be used to eliminate the first-order Doppler width. The resonance line $4^2S_{1/2}$-$4^2P_{1/2}$ is strong enough to cool the ions by radiation pressure. However, the corresponding branching ratio to the $(n-1)$ D level $\left(\dfrac{A(^2P\text{-}^2S_{1/2})}{\sum_J A(^2P\text{-}^2D_J)} \right) = 17.6$ [14], requires recycling of the $3^2D_{3/2}$-state ions by using the 866 nm line. The fine structure transition of the D-levels at 1.89 THz can also be used as a frequency standard in the far i.r. region and finally the hyperfine structure of the fundamental level of $^{43}Ca^+$ at 3.2 GHz. An important quality of the Ca^+ system is that all the transitions involved in the optical domain are accessible by diode lasers. D-P transitions can be generated directly by using commercial diodes. The clock transition can be probed with a nitrogen-cooled laser diode. Recently, doubling of a high-power diode laser was demonstrated to produce the UV lines [15]. Otherwise, Ca^+ is of

Table I. — *Compilation of data on the first metastable* D-*levels in* CaII. *All the experiments were carried out with Paul traps.*

	Computed : (s)			Experiments : (s)			
Ref.	17	16	18	19	21	22	20
$^2D_{3/2}$	1.271	1.16	1.20	1.24(39)			1.113(45)
$^2D_{5/2}$	1.236	1.14	1.16	1.24(39)	0.77(7)	1.08(22)	1.054(61)

astrophysical interest (intense resonance line in the sun spectrum, E2-lines in Seyfert 1 galaxies, T Tauri stars and in Beta pictoris disk [16]) and precise spectroscopic data are required to build dynamic models for understanding these phenomena. Finally, knowledge of CaII oscillator strengths contributes to the understanding of the d orbital collapse with increasing nuclear charge.

The metastable $(n - 1)$ D-levels are now considered both theoretically and experimentally. Table I gives recent computations of the natural lifetimes by using relativistic many-body calculations with a third-order perturbation [17], a multiconfiguration Hartree-Fock (MCHF) method taking into account core-valence correlation [16], an improved MCHF method including a relativistic correction [18] as well as the experimental values. The latter are obtained from ion clouds at 2 000 K [19], at 8 000 K [20], with laser cooling on two to three ions at a temperature lower than 1 K [21], and on a single ion at 130 mK [22].

In spite of the fact that ultimate qualities for the optical transitions will be reached only in the presence of a few ions (or only one) with a highly-stabilised laser, we started by confining a Ca^+ ion cloud. The aim of this paper is to report on the interaction between the buffer gas and the atomic ions and to give our first results concerning the spectroscopic investigations. We present first our apparatus, secondly the properties of the stored ion cloud and finally we describe the experiments on the forbidden lines, which were performed from direct excitation of the D-levels followed by the pumping of the P-level from the metastable states. A qualitative study of the D-level fine-structure mixing is presented.

2. The r.f. ion storage technique and the experimental set-up.

Radiofrequency ion traps are capable of storing, in a small region of space, thanks to the large potential well depth available, small ion clouds in a well defined and well controlled environment, without a magnetic field, for long periods enabling accurate observations. Confinement [23, 24] is obtained by creating a quadrupole electric field, inside the trap, which results of the superposition of a direct voltage, V_{dc}, and of an alternating voltage, V_{ac}, at the radiofrequency $\Omega/2\pi$, in such a way that the motion amplitude stays finite for a set of values (V_{dc}, V_{ac}, Ω), which depends on the electron charge to ion-species mass ratio $\left(\frac{e}{m}\right)$ and the geometry of the device, r_0, z_0 (Fig. 2). This set of values constitutes the stability diagram. The usual reduced parameters are (for singly charged ions) :

$$a_z = \frac{-16\,eV_{dc}}{m\Omega^2(r_0^2 + 2z_0^2)}; \quad a_x = a_y = -a_z/2$$

$$q_z = \frac{-8\,eV_{ac}}{m\Omega^2(r_0^2 + 2z_0^2)} \qquad q_x = q_y = -q_z/2 \tag{1}$$

according to the electrical scheme in figure 2.

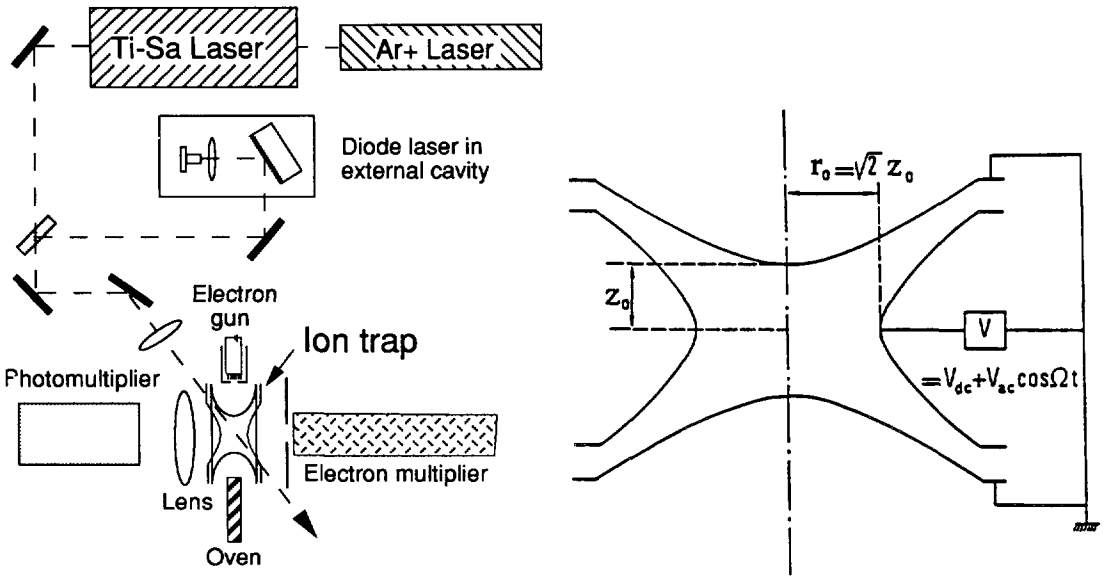

Fig. 2. — Experimental apparatus (a) and the r.f. ion trap (b).

Trapped ion motion is ideally quasiperiodic. For each component, with respect to the cylindrical revolution, the frequency spectrum contains the so-called fundamental frequency ω_1 (resp. ω_2), which is always smaller than the driving frequency, Ω. Higher harmonics are present at $\omega_1 \pm n\Omega$ (resp. $\omega_2 \pm n\Omega$). The most intense ones correspond to $n = 0$, ± 1 and, less important, to $n = 2$. Therefore, the motion is mainly the superposition of a secular motion at ω_1 (resp. ω_2) and a micromotion at Ω. Secular frequencies ω_1 (resp. ω_2) depend on the a_1 and q_1 (resp. a_2 and q_2) values, and they are obtained from the r.f. frequency Ω according to :

$$\omega_1 = \beta_1 \Omega/2\,, \qquad \omega_2 = \beta_2 \Omega/2 \qquad (\text{with} \quad 0 < \beta_1, \beta_2 < 1) \tag{2}$$

where β_1 (resp. β_2), can be approximated by $\sqrt{a_1 + \frac{1}{2}q_1^2}$ $\left(\text{resp. } \sqrt{a_2 + \frac{1}{2}q_2^2}\right)$ for small Mathieu parameters. Computations of more exact values must however use iterative methods [25].

The micromotion causes r.f. heating and is the main limitation for laser cooling with more than a few ions. Anharmonicities in the system, responsible for couplings between the secular and the micromotion or between the different degrees of freedom [26, 27] modify the frequency spectrum of each component of the motion. The investigation of these spectra can therefore give information on the ion dynamics and storage properties [26].

Ca^+ ions are stored in a conventional hyperbolic radiofrequency trap (Fig. 2) with $r_0 = \sqrt{2}\,z_0 = 7.2$ mm. The ring of the ion trap is made of stainless steel and the end caps from molybdenum mesh of high transmission (83 %). The experiment is performed under ultrahigh-vacuum conditions with residual pressures less than 10^{-9} mbar. A needle valve allows the introduction of a pure buffer gas, the pressure of which is measured by a linear quadrupole mass spectrometer and a Bayard-Alpert gauge. Ca atoms are evaporated into the trap from a small oven, situated very close to the ring (Fig. 2) and are ionised inside the trap with a pulsed

electron gun, which is biased at -40 V. The confinement radiofrequency Ω is equal to 1 MHz $\times 2\pi$, the dc voltage V_{dc} varies between 0 and 10 V and the ac voltage V_{ac} between 90 and 115 V. Working points are therefore close to the best conditions of storage [28, 29]. Besides optical detection (see below), Ca^+ ions can be detected electronically by resonant detection [30] which monitors the ion energy absorption in a circuit tuned to one of the motional frequencies, and by a resonant ejection method [31], by using an electronmultiplier. The latter can show the ion motion properties when ions are submitted to an additional dipole or quadrupole alternating voltage at variable frequency. Both methods can increase slightly the ion kinetic energy.

For spectroscopic investigations, the resonance radiations are generated by a titanium-sapphire ring laser (Coherent 899-05). The first harmonic is doubled by an intracavity $LiIO_3$ crystal which provides up to 19 mW at 397 nm, with a spectral width of 1 MHz. A laser diode, covered with an antireflection coating, is mounted in an external cavity (1 200 lines per mm Jobin-Yvon grating) and can be tuned between 845 and 867 nm with a spectral width of approximately 30 MHz. At 866 nm, the resulting power is estimated to be 200 μW. The 729 and 732 nm lines are available from the fundamental of the Ti-Sa laser with power up to 1 W. The laser beam traverses the trap diagonally between the ring and the caps. It is focussed at the centre of the trap giving a beam waist diameter w_0 of 70 μm for the 397 nm and of 150 μm for the red radiation. The diode laser beams, due to their divergence and astigmatism, are difficult to focus. They have a minimal diameter of about 0.5 mm inside the trap and they overlap the Ti-Sa laser beam. Emitted photons are collected by a large aperture aspherical lens and are focused on a Hamamatsu H4730 photo multiplier which is run in the photoncounting mode. To discriminate the signal from the background and the scattered photons, an interference filter can be placed in front of the photomultiplier.

3. Electronic and optical ion-cloud studies.

The properties of the ion cloud are firstly investigated with electronic methods. These methods are more reliable for long measurement periods than optical ones which require the laser power to be stable enough to precisely measure relative ion number variation, as the ion cloud evolves. Moreover, all the ions are subject to the electrical excitation and the signal is generally independent of the geometrical shape of the cloud.

Introduction of a light buffer gas into the apparatus can, due to elastic collisions, reduce the ion kinetic energy. This partially compensates the r.f. heating and therefore increases the confinement times. In the presence of helium at 10^{-6} mbar, ions are stored for several hours. The storage time depends on the buffer gas pressure and, as predicted, is optimised for a given pressure [32]. Other gases, such as nitrogen or neon, make the ion-cloud storage time shorter, as their masses are comparable to that of calcium. These observations are represented in figure 3.

Resonant ejection [31] with a quadrupolar tickle of 0.01 V during 10 ms shows peaks at $\omega_r/2$, ω_r, ω_z, $\omega_z + \omega_r/2$, $2\omega_z - \omega_r$, $\omega_r + \omega_z$, $2\omega_z$ (Fig. 4). The measured secular frequencies (contrary to the theoretical values) depend on the coupling parameters (space charge, anharmonicities). The space charge effects are related to the collisions with the buffer gas. Indeed, with light buffer gases, the collisions reduce the kinetic energy [30, 33] and increase the Γ coupling factor [34] ($\Gamma = \dfrac{e^2}{4\pi\varepsilon_0 akT}$, where k is the Boltzmann constant, T the ion temperature, defined below, and a is the mean distance between the ions such that $\dfrac{4\pi n_0 a^3}{3} = 1$, with n_0 the ion density at the center of the trap). The secular frequencies also are strongly shifted to lower values [35]. These reductions can be seen as a reduction of the β

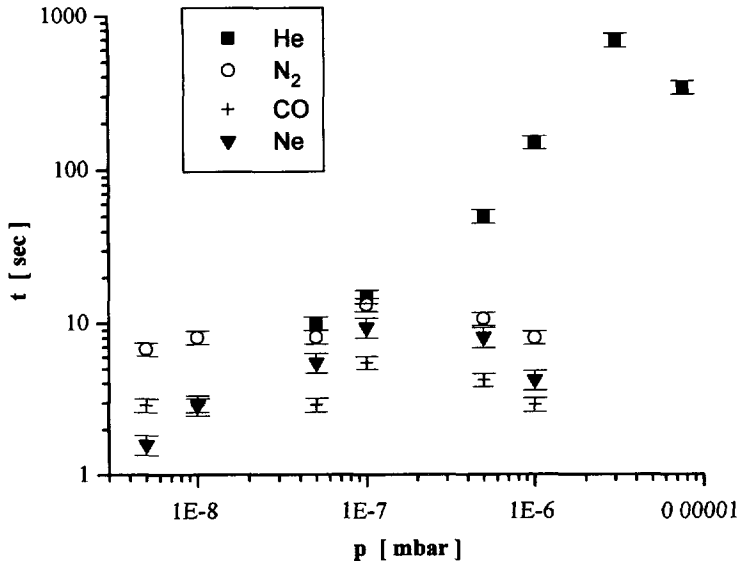

Fig. 3. — Storage time as a function of buffer gas pressure.

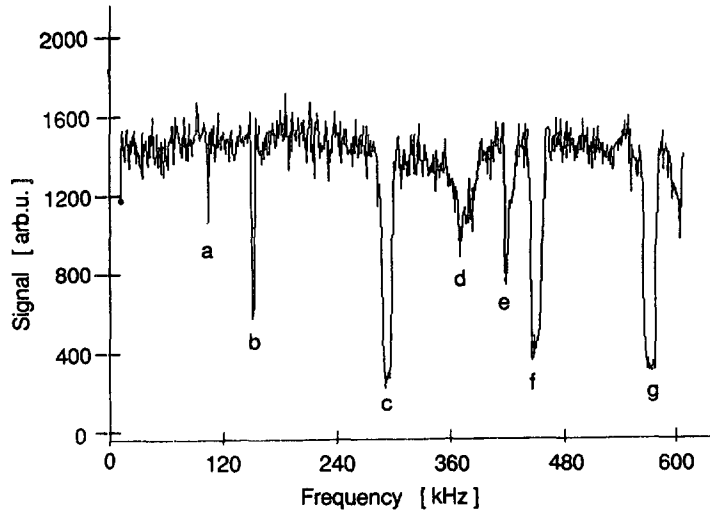

Fig. 4. — Ion ejection signals in the presence of a quadrupolar excitation. The signal is observed with a delay after the electric excitation and when the confinement voltage is just interrupted in such a way that the spectrum is relevant from the axial and radial motion spectrum. a) $\omega_r/2$, b) ω_r, c) ω_z, d) $\omega_z + \omega_r/2$, e) $2\,\omega_z - \omega_r$, f) $\omega_r + \omega_z$, g) $2\,\omega_z$.

parameters or a displacement in the stability diagram. Therefore, if observations are made with the resonant electronic detection (where the signal is obtained by working with a fixed resonance) the dc-voltage has to be decreased in order to compensate the displacement of the working point in the stability diagram. Figure 5 gives a good illustration of such an evolution of the cloud *versus* the buffer-gas pressure, as well as the influence of the neutral/ion mass ratio. Apparently, collisions with nitrogen molecules have almost no effect on the kinetic

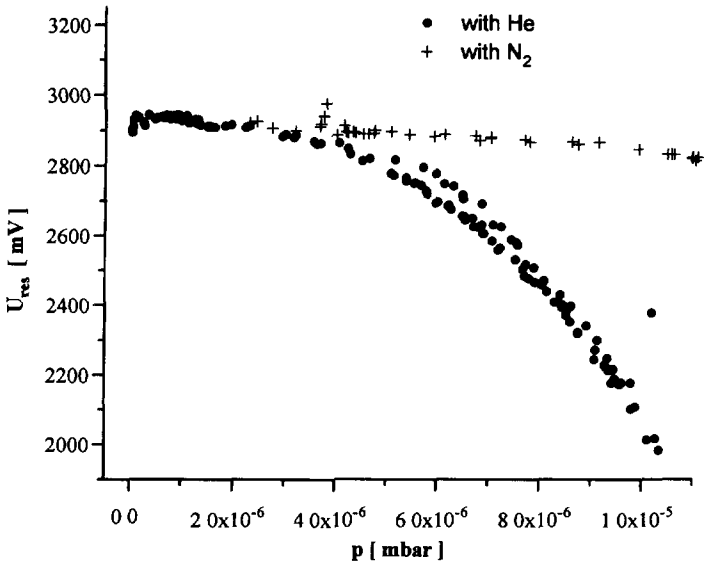

Fig. 5. — Variation of confinement parameters *versus* the pressure, due to space charge, by using different buffer gases.

energy nor on the shape of the cloud. It can be observed that the variation is weaker when the pressure is lower since Γ is smaller (because the buffer gas cooling is less efficient).

Collisions with the background gas lead very quickly to relaxation. Once equilibrium is reached, collisions allow some ions to escape. This ion loss is generally observed as exponential and implies that the cloud behavior depends on time. An observed decrease at 3×10^{-6} mbar is shown in figure 6. Due to the decrease of the ion number, space charge diminishes and the working point moves for the same reason as in figure 5.

Our first optical detection of the ions uses the u.v. fluorescence signal due to the excitation of the P level. Owing to the high branching ratio of 17.6 between the S and the D-level and the

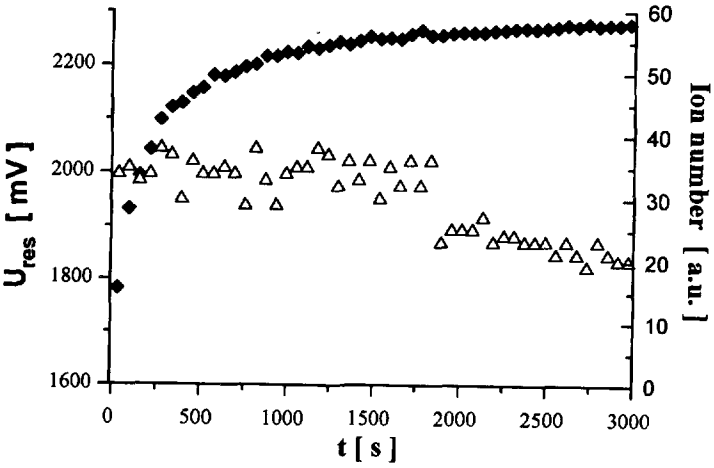

Fig. 6. — Temporal evolution of space charge (♦) and ion loss (△), the time constant for the latter is of the order of magnitude of one hour.

long lifetime of the metastable states, ions are trapped in the D-state. However, observation of a fluorescence signal is possible by the presence of a buffer gas which reduces the D-lifetime by quenching.

The addition of a diode laser, which empties the D-level and permits all the ions to be involved in the absorption/emission cycle, allows a drastic increase of the signal-to-noise ratio as seen in figure 7.

The Gaussian character of the ion velocity distribution is well established experimentally [36] as well as theoretically [33, 37]. The distribution for each component (with respect to the cylindrical symmetry) oscillates at the radiofrequency. Its width depends on the working point (micromotion amplitude), the potential well depth and, as already mentioned, on the neutral-to-ion mass ratio. Although already used in this presentation, the notion of temperature applied to a stored ion cloud must now be defined. The r.f. time-average of the mean kinetic energy commonly allows definition of an *axial* or *radial temperature*. This parameter can be checked either with electronic detection as in time-of-flight experiments [38-40] or with optical measurements. In the case of optical measurements, the temperature can be deduced from the Doppler profile obtained by sweeping the laser frequency. The temperature has to be deduced from the standard deviation which corresponds to a profile of the velocity distribution *versus* one degree of freedom. Since the laser crosses the ion trap diagonally, the profile is related to the projection of the three components of the ion motion. The standard deviation of the observed Gaussian profile σ_{obs} is given from the standard deviations for each component :

$$3\,kT/m = \sigma_r^2 + \sigma_\perp^2 + \sigma_z^2 = \sigma_{obs}^2(2\sin^2\varphi + \cos^2\varphi) \qquad (3)$$

where φ is the angle between the laser beam and the revolution axis of the ion trap. In our experiment, φ is equal to 38° and $3\,kT/m \approx 1.4\,\sigma_{obs}^2$.

Ion motions are coupled together by the anharmonicities of the fields and space charge, which permits the assumption that the velocity distribution is isotropic. Ideally (pure quadrupole field without parasitic coupling) the anisotropic property defined by $\sigma_z/\sigma_\perp$ does not exceed, for our (a_z, q_z) values, 1.3 [41].

The efficiency of the collisional cooling was monitored by observation of the Doppler profile and controlled by buffer gas pressure. The evolution of temperature can be seen in figure 8.

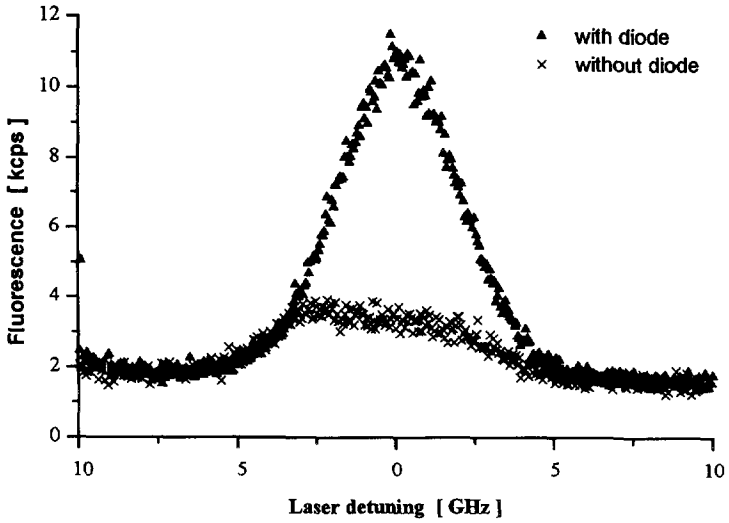

Fig. 7. — Detected resonance line at 397 nm : (×) only with a buffer gas, (▲) in double resonance.

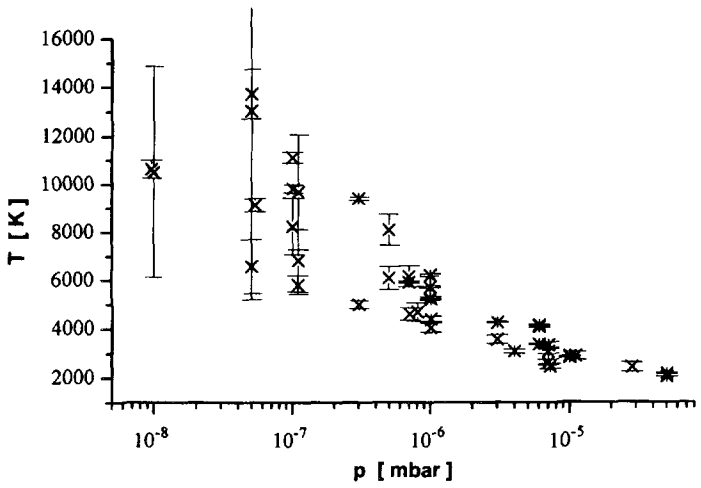

Fig. 8. — Temperature of the ion cloud as a function of helium buffer gas pressure ; at lower pressures, the signal to noise ratio diminishes due to the decreasing ion density.

Here the averaged kinetic energy is therefore 0.2 to 1 eV, for a total potential well depth ($D_r + D_z$) of 62 eV. Similar values were obtained for Ca^+ stored in a shallower potential well [19]. This confirms that the dependence of the kinetic energy *versus* the potential well depth is not simple [37]. The variation of the kinetic energy *versus* the pressure should be considered for rate constant studies.

4. Direct excitation of the E2-transitions.

Because of the strong interest for the 729 nm line as a frequency standard, the forbidden transitions were investigated. One of the D-levels was pumped directly by the first harmonic of the Ti-Sa laser. Simultaneously, the corresponding P-D transition was excited using the grating-stabilized diode laser at a fixed frequency. Detection was made on the S-P fluorescence at 397 nm, as discussed above. This pumping scheme has the advantage of eliminating the scattered photon background.

A typical profile of the 729 nm-line is shown in figure 9, with 700 mW of laser power (because of the smaller linewidth, lower power will be required for colder clouds). In spite of the relatively weak count rate, the signal/noise ratio (close to 10) allows us to use direct pumping of the D-levels in order to investigate them. For the excitation of the electric quadrupole transition, the available laser power is much less than that needed for saturation, whereas for the D-P transition, the diode laser power far exceeds the saturation limit. In order to use this detection scheme for further experiments, its efficiency was tested over a broad range of helium pressures. It was observed that the signal grows rapidly when the pressure increases, with a slight background increase. This behaviour shows that collisions with the neutral particles concentrate the cloud and enhance the optical signal. Moreover, the width of the lines decreases due to the cooling effect. The temperature, which is deduced from this profile is very close to the values given above.

In the presence of helium (or other gases), the lifetimes of the metastable levels depend on the quenching and fine-structure mixing rates. Actually, besides the collisional relaxation, a strong mixing rate exists due to the small energy difference between the $D_{3/2}$ and $D_{5/2}$ levels

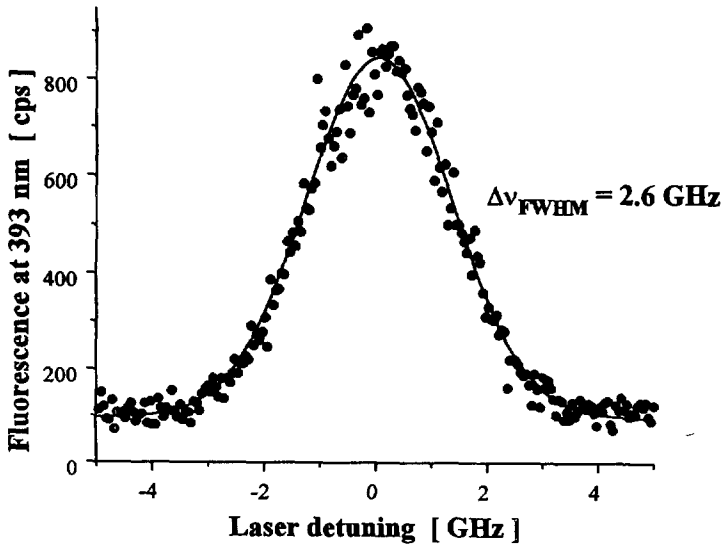

Fig. 9. — Observation of the electric quadrupole transition at 729 nm *via* the resonance line at 393 nm, at 2×10^{-6} mbar of helium pressure.

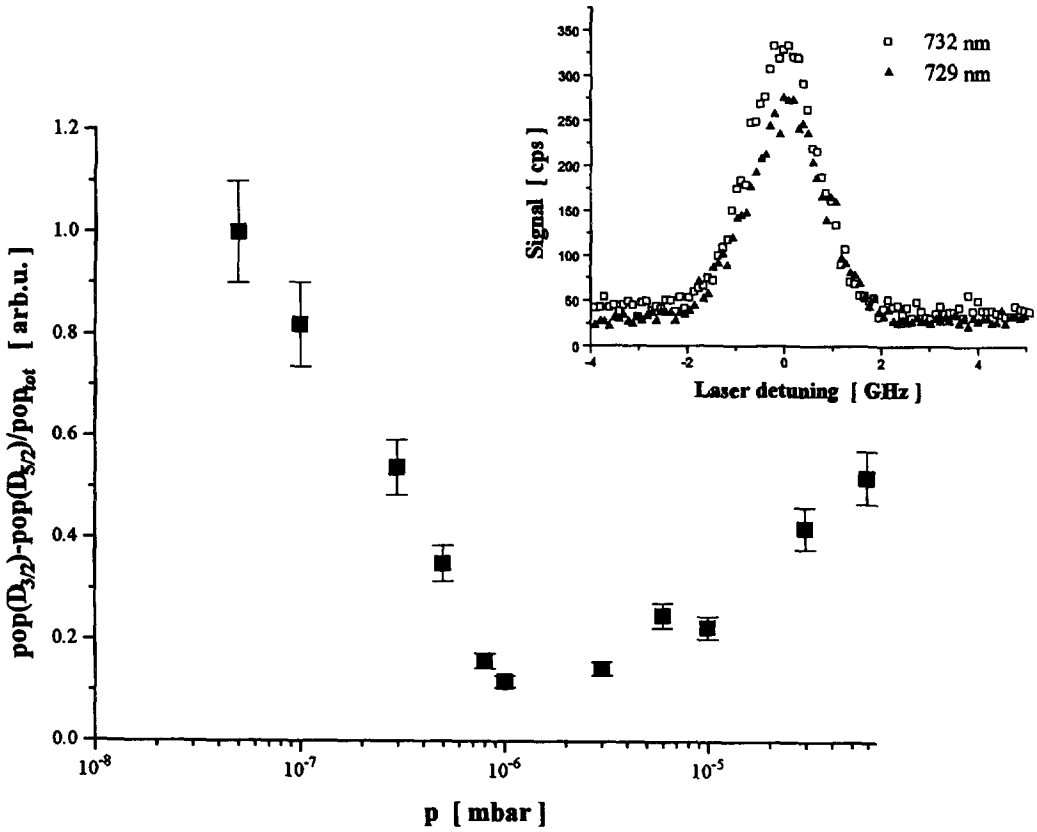

Fig. 10. — Population difference of the $3D_{5/2}$ and $3D_{3/2}$ levels as a function of buffer gas pressure. At 10^{-6} mbar, the levels are almost completely mixed. Inset : fluorescence intensities of both forbidden transitions, although only the $D_{3/2}$-state is directly populated at 2×10^{-6} mbar.

(7.4 meV) [19]. To study this we probed the $3^2D_{3/2}$ level by observing the resonance line at 397 nm from the $4^2P_{1/2}$ pumped with the diode laser at 866 nm. Excitation was made either at 732 nm ($4^2S_{1/2}$-$3^2D_{3/2}$), or at 729 nm ($4^2S_{1/2}$-$3^2D_{5/2}$). The normalized intensities of both lines (for which the difference between the oscillator strengths is very small) are quite comparable in the presence of helium at rather high pressures. Figure 10 shows the variation of the population differences *versus* the helium pressure in a large domain. It clearly demonstrates the dependence of the *j*-mixing with the pressure. A maximum exists around 10^{-6} mbar. Lower pressures reduce collisions and the *j*-mixing while, for higher pressures, the collisions increase the observed $D_{3/2}$ ion loss rate and shorten its lifetime considerably so that mixing can no longer take place.

5. Conclusion.

In order to study the potential of the high-Q line of CaII as a frequency standard in the optical domain, we began a spectroscopic study on stored Ca^+ ions.

We constructed an ion trap apparatus which can confine 10^4 to 10^5 Ca^+ ions and obtained experimental conditions for long storage. The direct excitation of the electric quadrupole transitions demonstrated a strong *j*-mixing which now must be quantitatively investigated. We intend to this by measurements resolved in time in the presence of gases besides helium, such as N_2, Ne. A quantitative study of the D-level lifetime and corresponding quenching and mixing rates by direct excitation of the metastable stages is underway [42]. The quenching and mixing rates should depend on the energy conditions, which can be changed by varying the working point.

Acknowledgments.

The authors would like to thank G. Werth, for encouragement and helpful discussions when starting this research and for access to the mechanical workshop in Mainz for the realisation of the ion trap. They also want to thank R. Thompson, for his efficient participation in the first optical measurements.

This work was supported by Direction Générale des Recherches et des Etudes Techniques. M. Knoop is grateful to the EC (Human Capital and Mobility program) for financial support.

References

[1] Dehmelt H., *Rev. Mod. Phys.* **62** (1990) 525-530.
[2] Werth G., *Jpn J. Appl. Phys.* **33** (1994) 1585-1589.
[3] Prestage J. T., Tjoelker R. L., Dick G. J. and Maleki, *J. Mod Opt.* **39** (1992) 221-232.
[4] Dicke R. H., *Phys. Rev* **89** (1953) 472-3.
[5] Wineland D. J. *et al.*, Laser Manipulation of Atoms and Ions, Int. School of Physics *Enrico Fermi*, Course CXVIII, E. Arimondo *et al.* Eds. (North Holland, 1992) pp. 539-552.
[6] Knab-Bernardini C., Knab H., Vedel F. and Werth G., *Z. Phys.-Atoms, Molecules and Clusters* **24** (1992) 339-342.
[7] Madej A. and Sankey D. J., *Phys. Rev. A* **41** (1990) 2621-2630.
[8] Nagourney W., Yu N., Dehmelt H., *Opt. Commun.* **79** (1990) 176-180.
[9] Madej A. A., Siemsen K. J., Sankey J. D., Clark R. F. and Vanier J., *IEEE Trans. Instrum. Meas.* **42** (1993) 234-241.
[10] Klein H. A., Bell A. S., Barwood G. P., Gill P. and Rowley W. R. C., *IEEE Trans. Instrum. Meas.* **40** (1991) 129-ff.
[11] Gerz C., Roths J., Vedel F. and Werth G., *Z. Phys.* **D 8** (1988) 235-238.

[12] Werth G., Possible precision far-infrared spectroscopy on trapped ions. Proceedings summer school « Applied Laser Spectros », W. Demtröder et M. Inguscio, Eds. (San Miniato, 1989).
[13] Plumelle F., Desaintfuscien M. and Houssin M., *IEEE Trans. Instrum. Meas.* **42** (1993) 462-466.
[14] Gallagher A., *Phys. Rev.* **157** (1967) 24-30.
[15] Hayasaka K., Watanabe M., Imajo H., Ohmukai R. and Urabe S., *Appl. Opt.* **33** (1993) 2387-2396.
[16] Vaeck N., Godefroid M. and Froese Fischer C., *Phys. Rev. A* **46** (1992) 3704-3716, and references therein.
[17] Guet C. and Johnson W. R., *Phys Rev. A* **44** (1991) 1531-1535.
[18] Brage T., Froese Fischer C., Vaeck N., Godefroid M. and Hibbert A., *Phys. Scripta* **48** (1993) 533-545.
[19] Arbes F., Gudjons T., Kurth F., Werth G., Marin F. and Inguscio M., *Z Phys* **D 25** (1993) 295-298.
[20] Arbes F., Benzing M., Gudjons T., Kurth F. and Werth G., *Z. Phys.* **D 29** (1994) 159-161.
[21] Urabe S., Watanabe M., Imajo H. and Hayasaka K., *Opt. Lett.* **17** (1992) 1140-1142.
[22] Urabe S., Hayasaka K., Watanabe M., Imajo M., Ohmukai R. and Hayashi R., *Appl Phys B* **57** (1993) 367-371.
[23] Paul W., *Rev. Mod. Phys.* **62** (1990) 531-ff.
[24] Wuerker R. F., Shelton H. and Langmuir R. V., *J. Appl. Phys.* **30** (1959) 342-349.
[25] Campbell R., Théorie Générale de l'équation de Mathieu (Masson, Paris, 1955).
[26] Vedel F. and Vedel M., *Phys. Rev. A* **41** (1990) 2348-2351.
[27] Vedel F. and Vedel M., Manipulation and detection of stored ions and applications to the study of ion/molecule reactions, in « Practical applications of Ion Trap Mass Spectrometry » Monographie C.R.C., in press, and references therein.
[28] Ifflander R. and Werth G., *Metrologia* **13** (1977) 167-ff.
[29] Vedel M., André J., Chaillat-Negrel S. and Vedel F., *J. Phys.* **42** (1981) 541-549.
[30] Dehmelt, H. G., *Adv. Atom. Mol. Phys.* **3** (1967) 53-72 ; **5** (1969) 109-ff.
[31] Vedel F., Vedel M. and March R. E., *Int. J. Mass Spectrom. Ion Proc.* **99** (1990) 125-138.
[32] Vedel M., *J. Phys. France Lett* **37** (1976) L339-340.
[33] André J. et Vedel F., *J. Phys. France* **38** (1977) 1381-1398.
[34] Bollinger J. J. and Wineland D. J., *Phys Rev. Lett.* **53** (1984) 348-351.
[35] Vedel F. and André J., *Phys. Rev. A* **29** (1984) 2098-2101.
[36] Schaaf H., Schmeling U. and Werth G., *Appl. Phys* **25** (1981) 249-251.
[37] Vedel F., *Int. J Mass Spectrom. Ion Processes* **106** (1991) 33-61, and references therein.
[38] Mosburg E. R., Vedel M., Zéréga Y., Vedel F. and André J., *Int J Mass Spectrom Ion Processes* **77** (1987) 1-12.
[39] Vedel F. and Vedel M., *Adv Mass Spectrom* (Heyden & Son, London) **11A** (1989) 244-245.
[40] Lunney M. D. N., Buchinger F. And Moore R. B., *J Mod Optics* **39** (1992) 349-360.
[41] Vedel F., André J., Vedel M. and Brincourt G., *Phys. Rev. A* **27** (1983) 2321-2330.
[42] Knoop M., Vedel M. and Vedel F., to be published.